LA-UR-17-29741
Approved for public release; distribution is unlimited.

Title: Aberrations and Emittance Growth in the DARHT 2nd Axis Downstream Transport

Author(s): Schulze, Martin E.

Intended for: Report

Issued: 2017-10-24

M. Schulze
5-October-2017

Aberrations and Emittance Growth in the DARHT 2nd Axis Downstream Transport

Introduction

The emittance of the DARHT 2nd Axis has been inferred from solenoid scans performed in the downstream transport (DST) region using a short kicked pulse. The beam spot size is measured by viewing optical transition radiation (OTR) in the near field as a function of the field (current) of a solenoid magnet (S4). The imaging station containing the OTR target is located about 100 cm downstream of the solenoid magnet. The emittance is then inferred using a beam optics code such as LAMDA or XTR by fitting the data to initial conditions upstream of the S4 solenoid magnet. The initial conditions are the beam size, beam convergence and emittance. The beam energy and current are measured.

In preparation for a solenoid scan, the magnets upstream of the solenoid are adjusted to produce a round beam with no beam losses due to scraping in the beam tube. This is different from the standard tune in which the beam tune is adjusted to suppress the effects of ions and rf in the septum dump. In this standard tune, approximately 10% of the beam is lost due to scraping as the beam enters the small 3.75" ID beam tube after the septum. The normalized emittance inferred from recent solenoid scans typically ranges from 600 to 800 π(mm-mrad).

This larger beam size increases the sensitivity to any non-linear fields in the Collins quadrupoles that are mounted along the small diameter beam tube. The primary magnet used to adjust the beam size in this region is the S3 solenoid magnet. Measurements made of the beam shape as the beam size was decreased showed significant structure consistent with non-linear fields. Using the measured magnetic fields in the Collins quadrupoles including higher order multipoles, the beam transport through the Collins quadrupoles is simulated and compared to the observed OTR images. The simulations are performed using the beam optics codes TRANSPORT [1] and TURTLE [2]. Estimates of the emittance growth and beam losses are made as a function of the S3 magnet setting. The increase in the spot size on the x-ray production target resulting from this emittance growth is examined for different DST tunes.

Layout and Optics

A schematic layout of the DST showing the relative magnet locations, imaging station beam dump and target is shown in Figure 1. The long pulse beam enters the kicker and is transported to the beam dump by the bias dipole which deflects the beam downward by 1-1.5^o. The beam enters the vertically defocusing septum quadrupole off axis to produce a net deflection of about 15^o. The dipole magnet further deflects the beam by an additional 30^o. For transport to the target the kicker is triggered to offset the deflection of the bias dipole so that the beam enters the septum quadrupole on axis and is not deflected. The kicker pulse length and voltage are adjustable.

The septum quadrupole produces an elliptical beam and the purpose of the Collins quadrupoles is to recover a round beam. The Collins quadrupoles are also used to minimize the effect of the rise and fall of the kicker pulse by tuning for point-to-point optics in the vertical plane from the kicker to the target [3]. The solenoids, S3 and S4 are used to adjust the size of the beam envelope in the DST. S4 is also used to perform studies at the imaging station such as solenoid scans to infer the beam emittance. The primary function of S3 is to match the beam from the accelerator to the downstream transport. This is accomplished by tuning the beam for a waist at the entrance to the septum quad. This results in a small

beam in the small aperture (3.75" D) region of the Collins quadrupoles. Unfortunately, a large beam size is required in the beam dump in order to minimize ion-backstreaming and associated problems [4]. This is required when Axis 2 is operated for four-pulse radiography and results in large beam sizes and associated beam losses in the small aperture Collins quadrupoles.

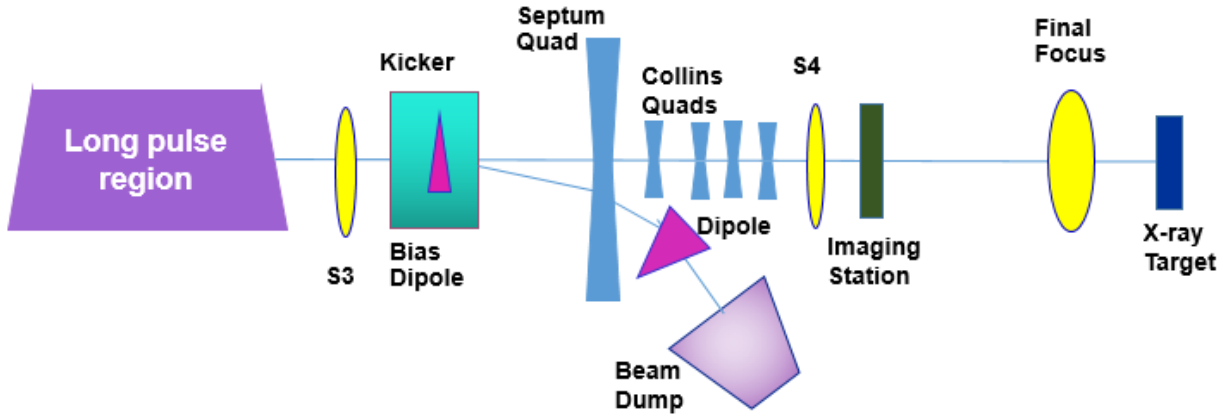

Figure 1: Schematic layout of the DST showing the relative magnet locations, imaging station beam dump and target.

Experimental Observations and Measurements

Beam studies at Station C are generally performed using a single pulse with the main accelerator pulse shortened. This avoids the need to make the beam large because the problems associated with ion-backstreaming are not observed for short pulses. Starting with a nominal target tune used for four-pulse radiography, the field in the S3 solenoid was lowered as the beam size was measured at Station C. Starting with a S3 setting of 76 A the current was lowered to 66 A in steps of 2 A until the beam transmission was essentially 100%. Figure 2 shows the beam transmission as a function of the S3 current. The beam profile measured at Station C is shown in Figure 3. The S4 solenoid was set to 44 A for these shots.

A particularly striking feature of these images is observed when the horizontal and vertical distributions are plotted. The distributions exhibit very sharp edges similar to uniform distributions. Figures 4-10 show the horizontal and vertical projections as well as line-outs of the distributions corresponding to S3 settings of 76, 74, 72, 70, 68, 66 and 64 A respectively. Examination of the horizontal and vertical projections as the field in the S3 solenoid is reduced shows that the distributions become more Gaussian. The strongly suggests that the shape of the distributions are sensitive to the size of the beam in the Collins quadrupoles. The histograms of the line-outs show that the distributions still exhibit sharp edges and are somewhat uniform even at the lowest S3 settings.

As described below, measurements of the Collins quadrupoles show significant nonlinear fields which can distort the particle trajectories by over focusing particles that are near the edge of the beam tube. An example of the effect of the nonlinear fields is shown in Figure 11 which shows a phase ellipse in the absence of nonlinear fields (red) and a distorted phase ellipse caused be nonlinear fields. The "folding" of the edges of the distribution will result in distributions such as those seen ion Figures 4-10. In addition, there will be significant emittance growth due to the distorted phase ellipse as the effective emittance will be that of an ellipse that encompasses the entire distribution as shown by the green ellipse whose emittance is 20% larger than the red ellipse.

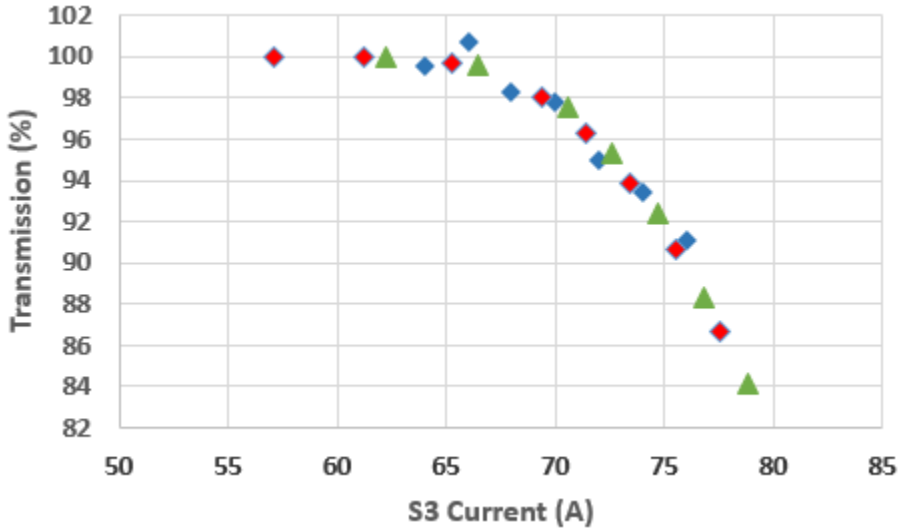

Figure 2: Beam transmission as a function of the S3 current. The blue diamonds are the measured transmission and the red diamonds and green triangles are from a TURTLE model of the DST as described below.

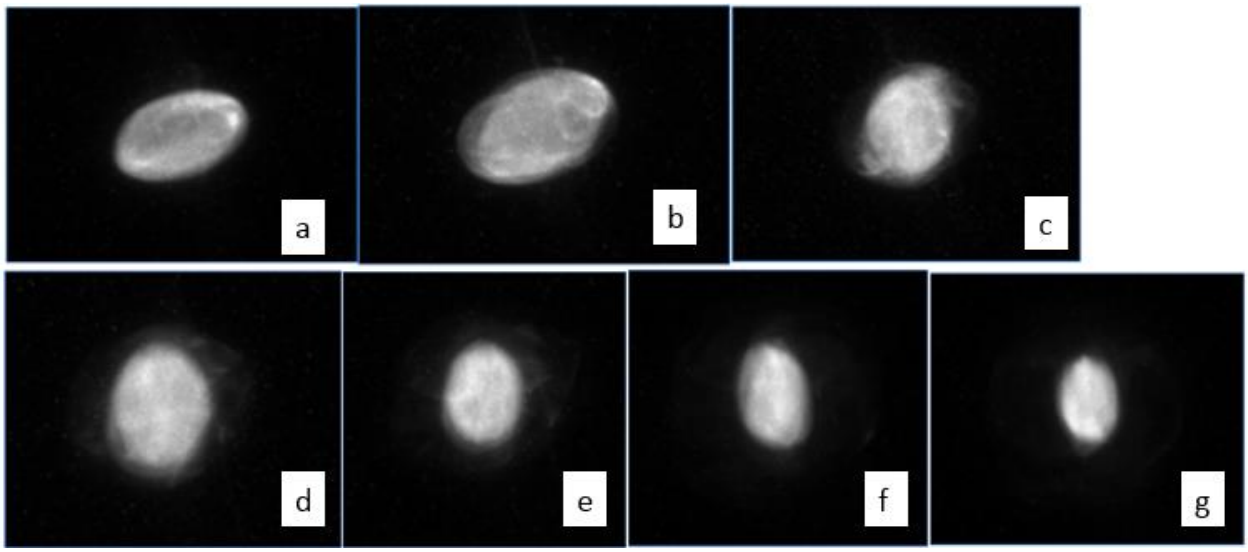

Figure 3: Beam profile as a function of the S3 current. Images a-g correspond to S3 settings of 76, 74, 72, 70, 68, 66 and 64 A respectively.

Measurements of the Collins quadrupoles show significant octupole (n=3) and duodecapole (n=6) field harmonics [5]. The measurements were made for the integrated field and the central field. POISSON [6] was also used to calculate the harmonics of the central field. Table 1 show the results of the measurements and simulations for the octupole and duodecapole fields as well as the n=10 pole. The measured and calculated values for the duodecapole component of the central field are in good agreement. The aberrations are dominated by the duodecapole field which is an order of magnitude higher than the other multipoles at a radius of 4 cm.

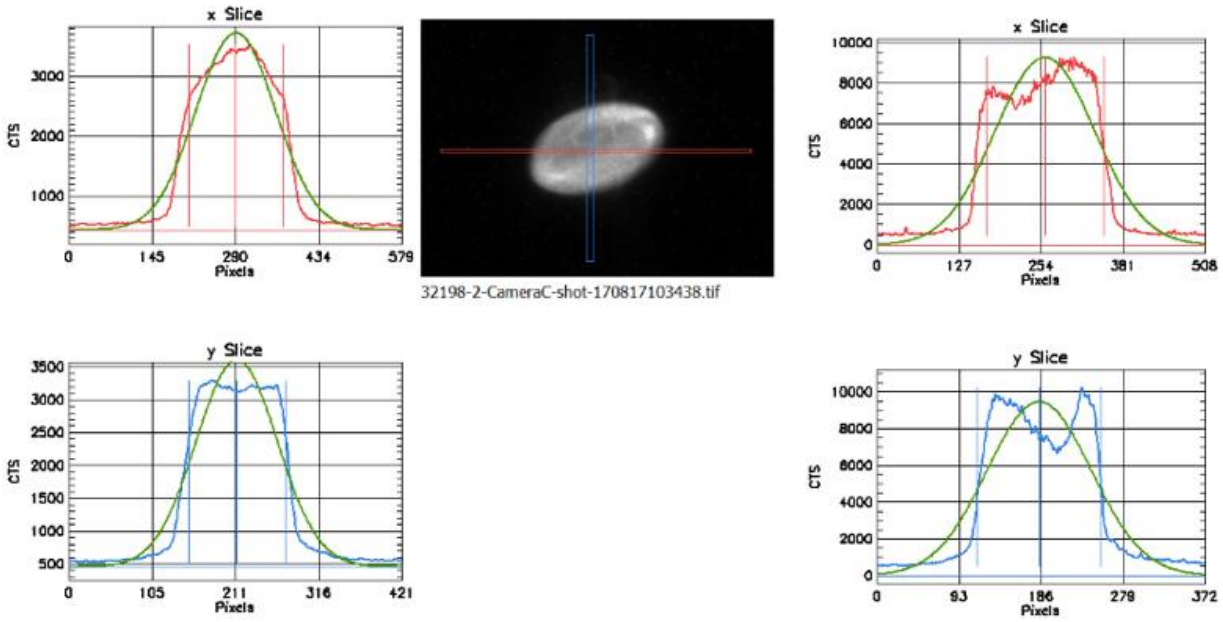

Figure 4: Horizontal and vertical projections of the Station C image for a S3 current of 76 A. The plots on the left are for the full distribution and those on the right correspond to the line-outs shown on the image. The green curves are a Gaussian fit to the distribution with the same FWHM.

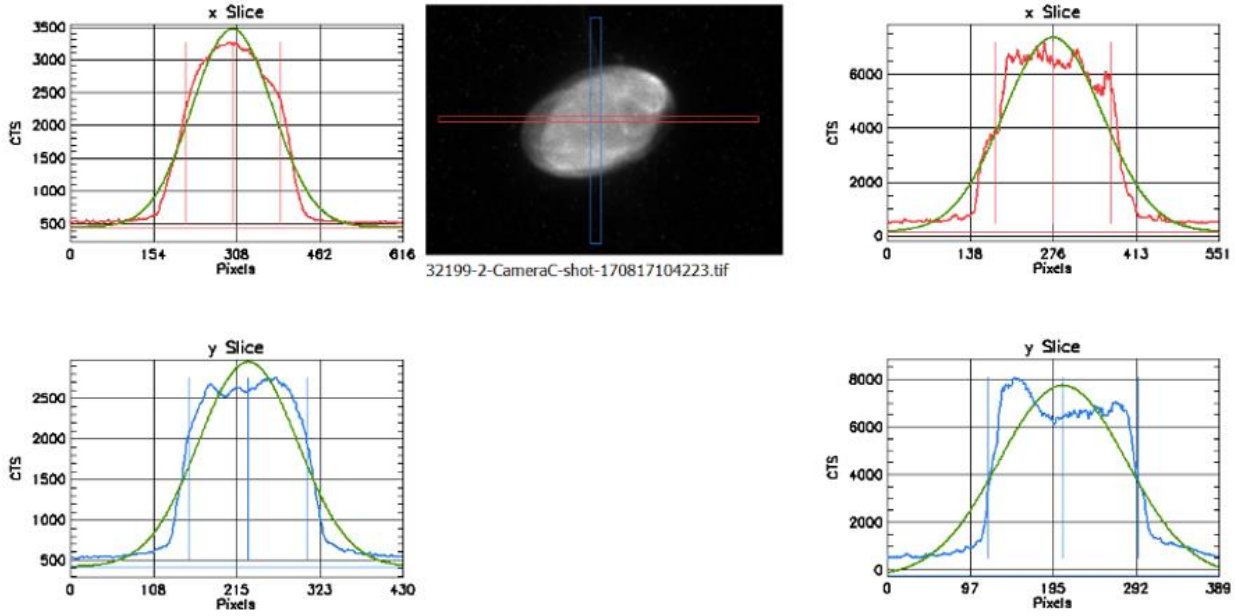

Figure 5: Horizontal and vertical projections of the Station C image for a S3 current of 74 A. The plots on the left are for the full distribution and those on the right correspond to the line-outs shown on the image. The green curves are a Gaussian fit to the distribution with the same FWHM.

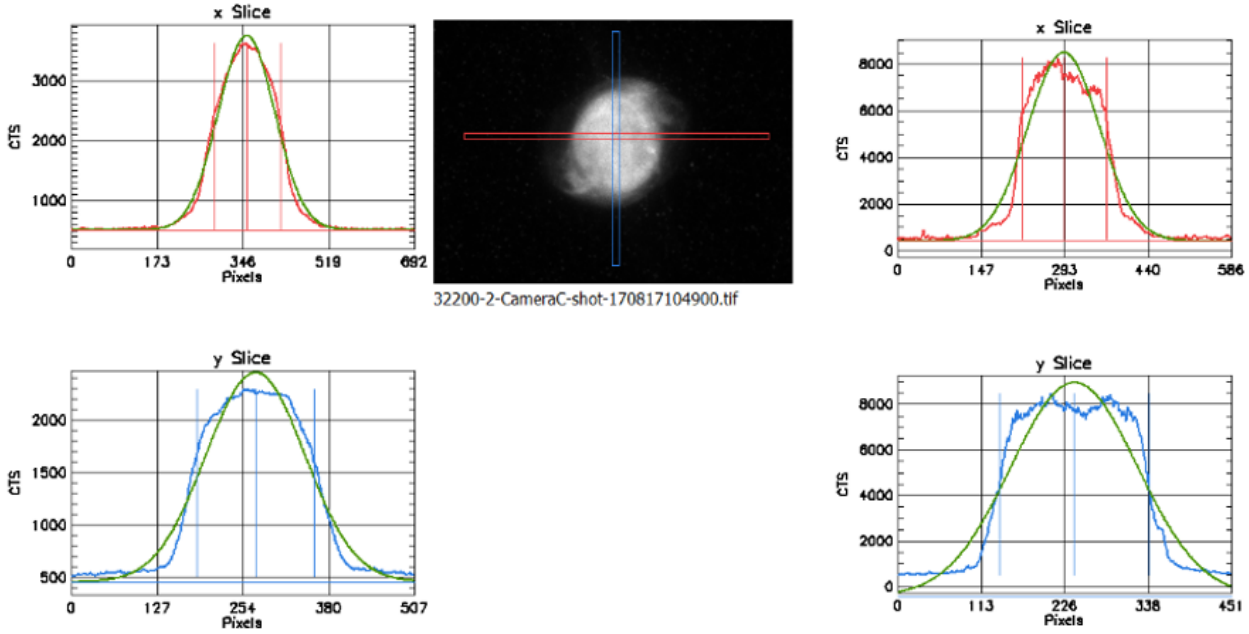

Figure 6: Horizontal and vertical projections of the Station C image for a S3 current of 72 A. The plots on the left are for the full distribution and those on the right correspond to the line-outs shown on the image. The green curves are a Gaussian fit to the distribution with the same FWHM.

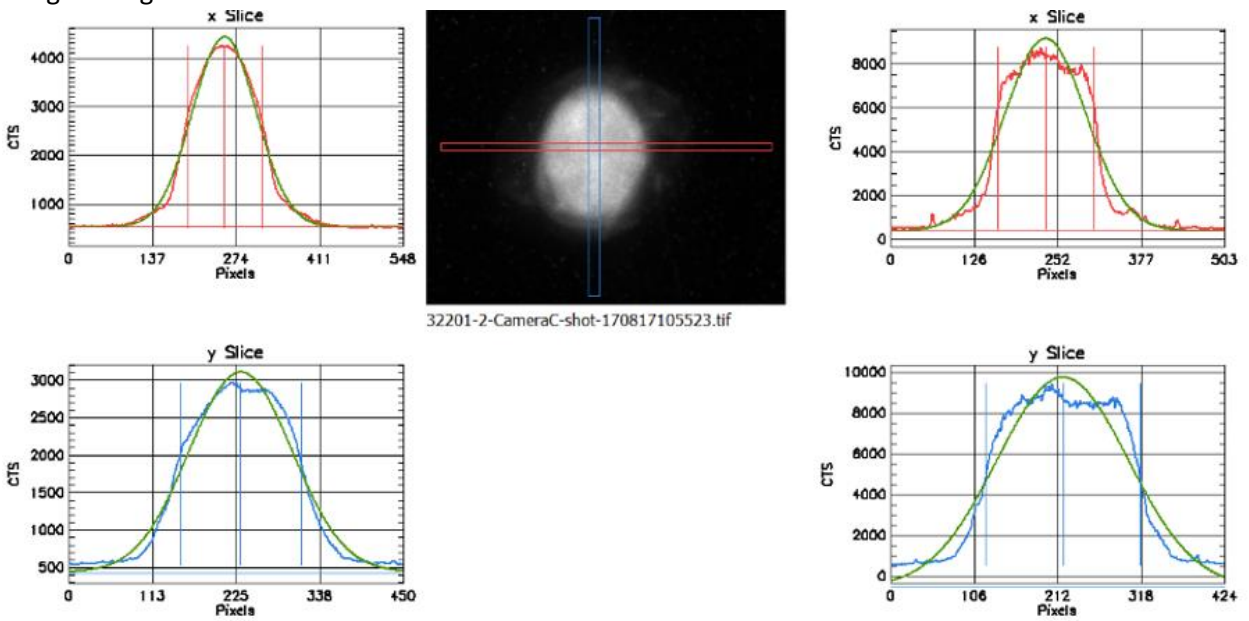

Figure 7: Horizontal and vertical projections of the Station C image for a S3 current of 70 A. The plots on the left are for the full distribution and those on the right correspond to the line-outs shown on the image. The green curves are a Gaussian fit to the distribution with the same FWHM.

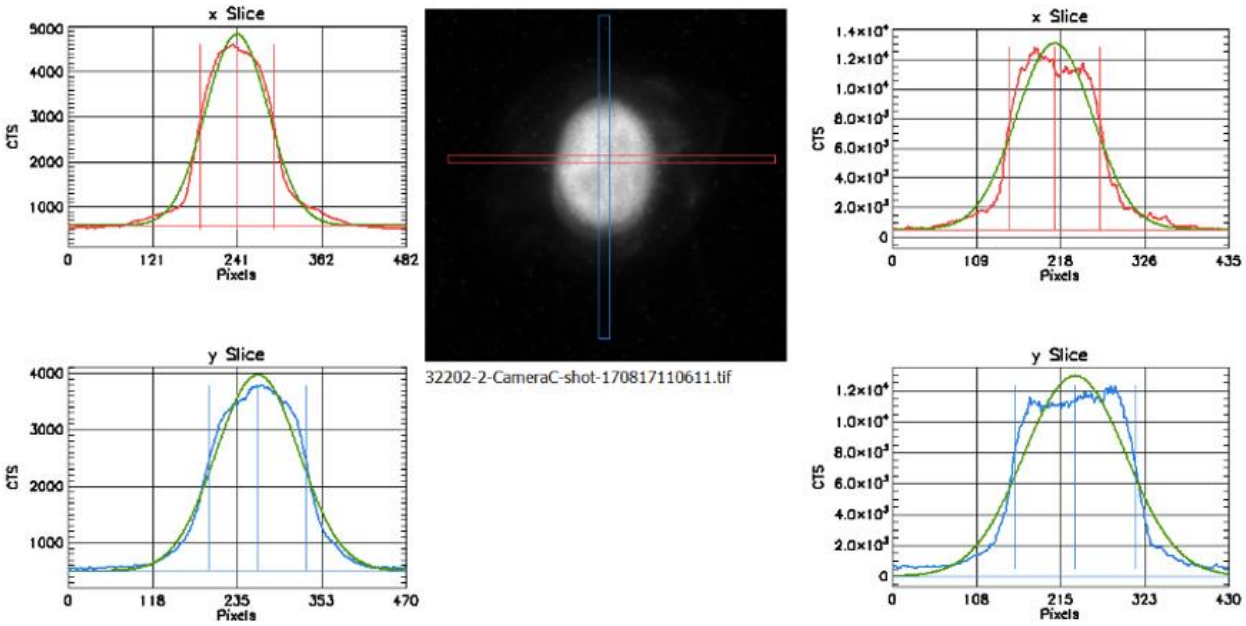

Figure 8: Horizontal and vertical projections of the Station C image for a S3 current of 68 A. The plots on the left are for the full distribution and those on the right correspond to the line-outs shown on the image. The green curves are a Gaussian fit to the distribution with the same FWHM.

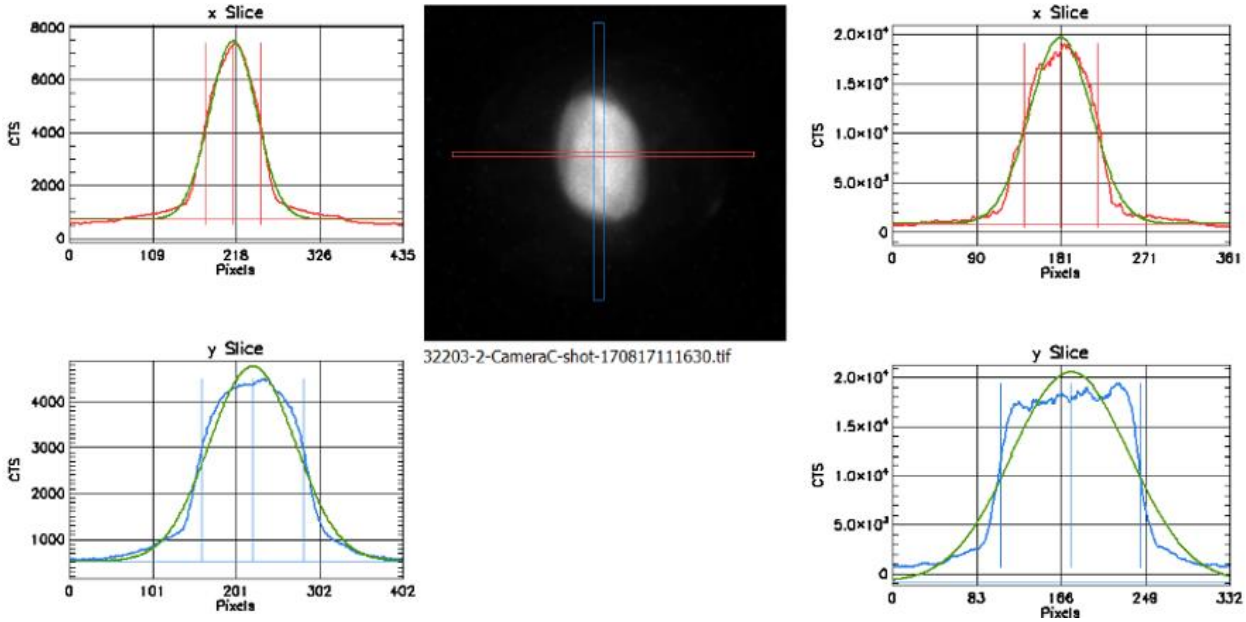

Figure 9: Horizontal and vertical projections of the Station C image for a S3 current of 66 A. The plots on the left are for the full distribution and those on the right correspond to the line-outs shown on the image. The green curves are a Gaussian fit to the distribution with the same FWHM.

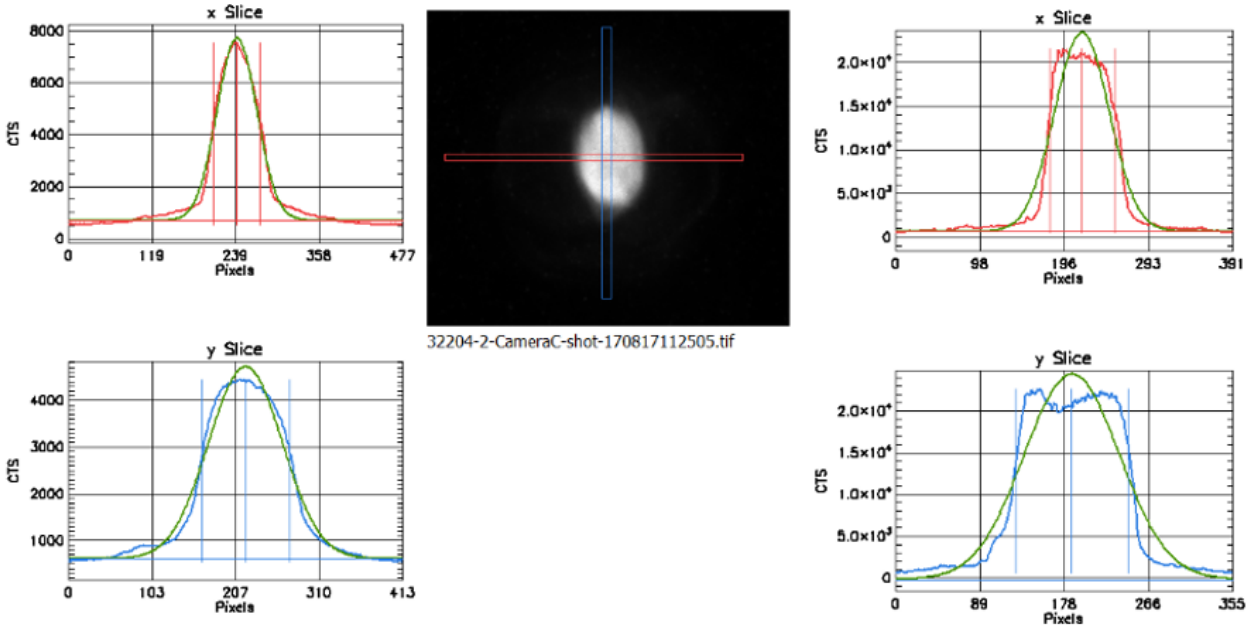

Figure 10: Horizontal and vertical projections of the Station C image for a S3 current of 64 A. The plots on the left are for the full distribution and those on the right correspond to the line-outs shown on the image. The green curves are a Gaussian fit to the distribution with the same FWHM.

Figure 11: Illustration of a 2-D phase space plot showing a normal ellipse (red) and a distorted ellipse (blue) due to the presence of higher order field aberrations. The green ellipse represents the ellipse that encompasses the distorted ellipse.

Table 1: Multipole components in the Collins quadrupole magnet as a percentage of the quadrupole at a radius of 4 cm

Multipole	Integrated	Central Measured	Central Calculated
octupole	0.28	0.31	0.01
duodecapole	3.23	2.61	2.5
n=10	0.19	0.17	0.69

TURTLE Simulations for Different S3 Currents

TURTLE has been used in an attempt to demonstrate that the higher order multipole fields in the Collins quadrupoles are indeed responsible for the structure in the measured beam profiles shown in Figures 4-10. The magnets, S3, SQ, CQH, CQV, CQW and S4 were adjusted, starting with the beam tune that corresponding to Figures 4-10. CQH, CQV and CQW are the first three Collins quadrupoles. Adjustments were required because TURTLE does not include space charge. Apertures corresponding to the 3.75" diameter beam tube were placed in the TURTLE beam line and the transmission was calculated as shown in Figure 2. The green triangles and red diamonds are for normalized beam emittances of 600 and 800 π(mm-mrad) respectively. A very good fit to the measured transmission is obtained for an emittance of 600 π(mm-mrad). The calculations made for an emittance of 800 π(mm-mrad) used a scaling factor that is 2% higher than the actual S3 current setpoint to achieve an equally good fit. Each of these simulations of the transmission provide a decent fit to the measured transmission and are supportive of the inferred emittance of 600-800 π(mm-mrad).

Figures 12-19 show the simulated beam distributions at imaging station C for different values of the S3 current ranging from 75.9 A to 55.9 A. The horizontal and vertical beam profiles show significant structure due to the higher order multipoles at the higher current as evidenced by the sharp edges of the distributions. As the beam size is reduced in the 3.75"D beam tube the effect of the higher order multipoles decreases and the beam becomes Gaussian corresponding to the initial beam distribution. No attempt was made to precisely match the beam distributions in Figures 4-10. Qualitatively, there is excellent correlation with the measured distributions presented in Figures 4-10 in that the shape of the distributions becomes more Gaussian as the beam size in the Collins quadrupoles is reduced and the transmission is increased. The horizontal distribution begins to more closely resemble a Gaussian at higher S3 currents in Figures 12-19 similar to the measurements in Figures 4-10.

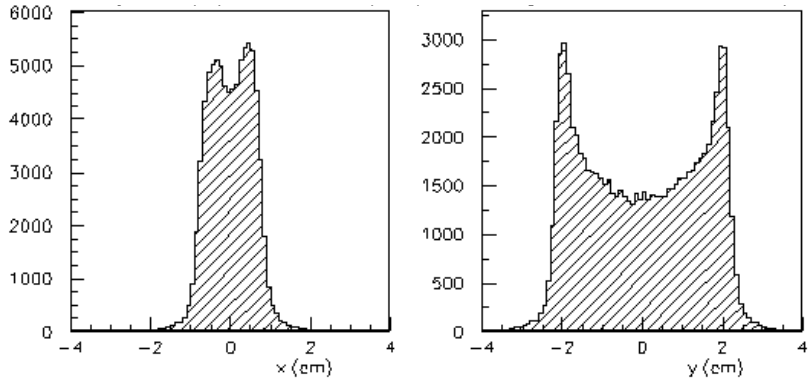

Figure 12: TURTLE simulation of beam profile at Station C for a S3 current of 75.9 A. The histogram on the left (right) is the projection on the horizontal (vertical) axis.

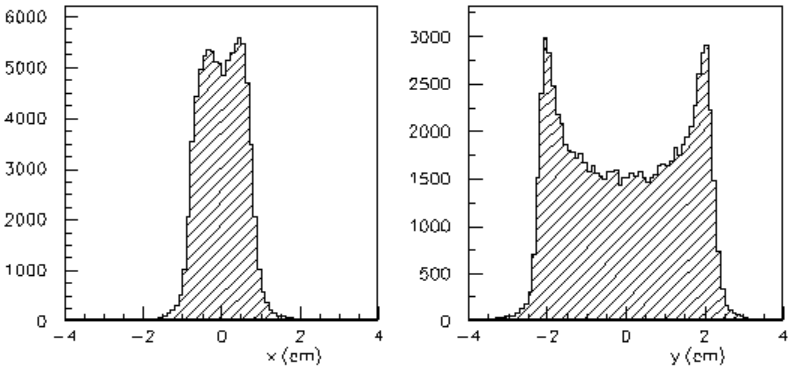

Figure 13: TURTLE simulation of beam profile at Station C for a S3 current of 73.9 A. The histogram on the left (right) is the projection on the horizontal (vertical) axis.

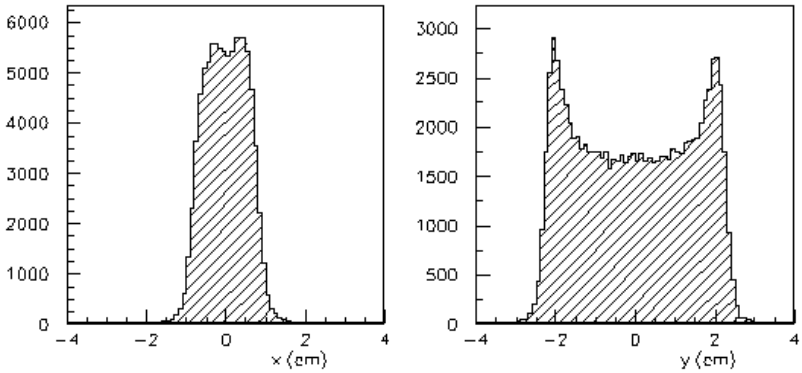

Figure 14: TURTLE simulation of beam profile at Station C for a S3 current of 71.9 A. The histogram on the left (right) is the projection on the horizontal (vertical) axis.

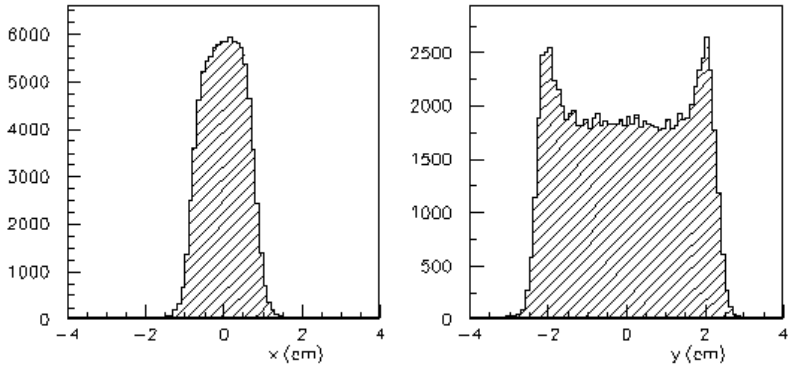

Figure 15: TURTLE simulation of beam profile at Station C for a S3 current of 69.9 A. The histogram on the left (right) is the projection on the horizontal (vertical) axis.

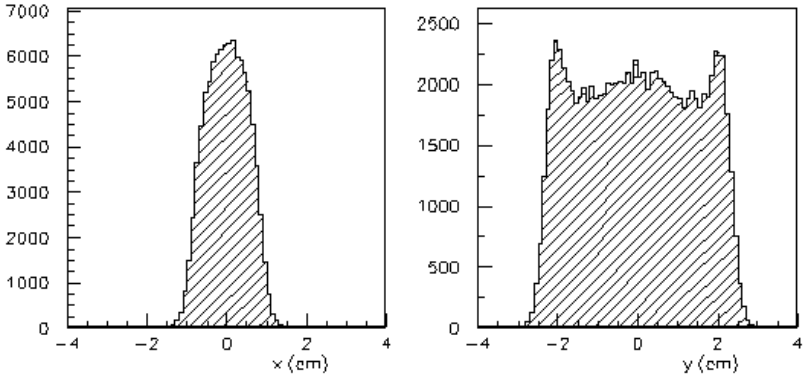

Figure 16: TURTLE simulation of beam profile at Station C for a S3 current of 67.9 A. The histogram on the left (right) is the projection on the horizontal (vertical) axis.

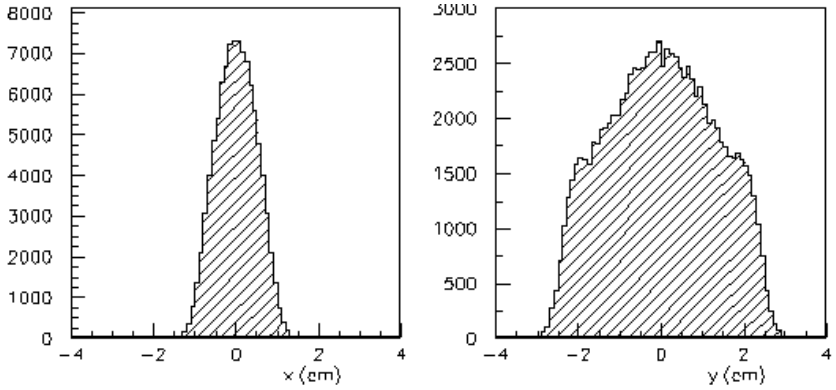

Figure 17: TURTLE simulation of beam profile at Station C for a S3 current of 63.9 A. The histogram on the left (right) is the projection on the horizontal (vertical) axis.

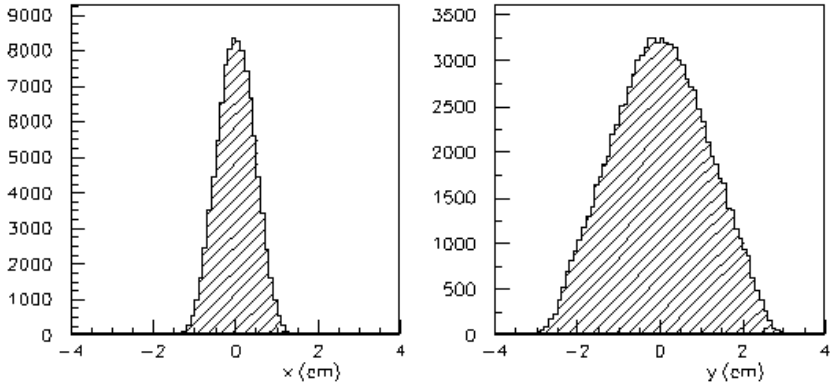

Figure 18: TURTLE simulation of beam profile at Station C for a S3 current of 59.9 A. The histogram on the left (right) is the projection on the horizontal (vertical) axis.

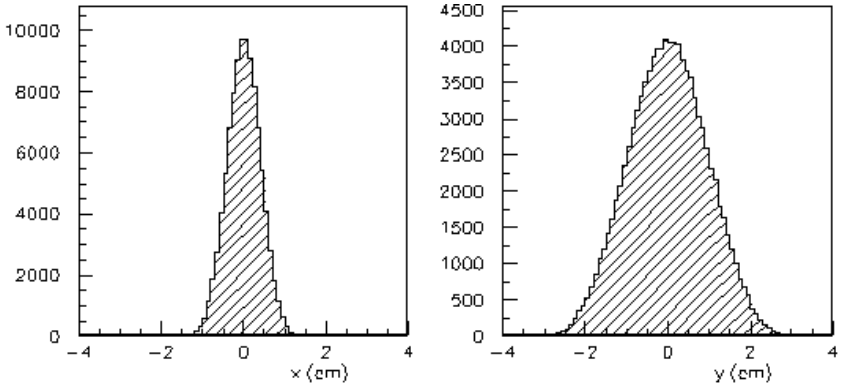

Figure 19: TURTLE simulation of beam profile at Station C for a S3 current of 55.9 A. The histogram on the left (right) is the projection on the horizontal (vertical) axis.

Emittance Growth and Target Spot Size

TRANSPORT is used to fit the magnetic fields in the Collins quadrupoles and produce a round beam with an rms radius just upstream of the final focus solenoid. The fit is for a S3 central field of 1.6 kG corresponding to a current of 63.9 A. The normalized beam emittance is 800 π(mm-mrad). The rms beam envelope is shown in Figure 20. These magnet settings are then used in TURTLE simulations.

Figures 21-26 show the horizontal and vertical phase ellipses for this tune for settings of the S3 solenoid corresponding to central fields of 1.4, 1.5, 1.6, 1.7, 1.8 and 1.9 kG respectively. The phase ellipses are from TURTLE simulations at the location of Station C. The contour lines show the relative shape of the center and edges of the distributions. The vertical phase ellipse is particularly distorted due to the large vertical beam size entering the Collins quads as seen in Figure 20. There is much less distorting in the horizontal plane. The S4 magnet is not turned on in these simulations. TURTLE calculates the area of the phase ellipses presented in Figures 21-26. These are plotted in Figure 27. The vertical emittance is seem to increase by a factor of 3.1 and the horizontal emittance increases by a factor of 1.6. The predicted emittance growth at the nominal S3 operating point of 76 A is a factor of about 1.4 and 2.7 for the horizontal and vertical planes respectively.

Figure 27 shows the simulated spot size on target as a function of the S3 setting for three values of the S4 current. The spot size on target is seen to almost double due to the aberrations in the Collins quadrupoles. The predicted increase in the spot size at the nominal S3 operating point of 76 A is a factor of about 1.7 to 1.9. These spot sizes are consistent with actual measurements.

These simulations suggest that the spot sizes on target can be substantially improved if the beam size is reduced in the Collins quadrupoles. A TRANSPOT solution showing such a tune is presented in Figure 28. This represents the nominal DST tune where a small waist is created at the entrance to the septum quad (SQ). Unfortunately, until the problems with the ions and rf are resolved, such a tune cannot be fully tested for four pulse radiography. It is possible however to test this tune with a single kicked pulse and measure the improvement in the spot size.

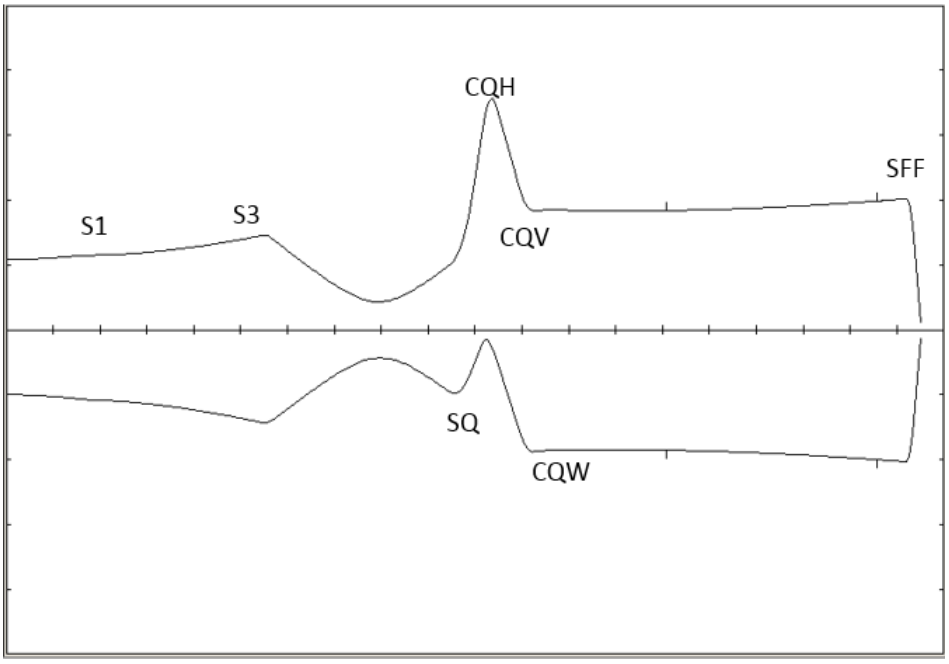

Figure 20: TRANSPORT fit of the DST to achieve a round beam with a rms envelope of 2 cm upstream of the final focus. The magnet locations are identified. The horizontal (vertical) envelope is shown on top (bottom).

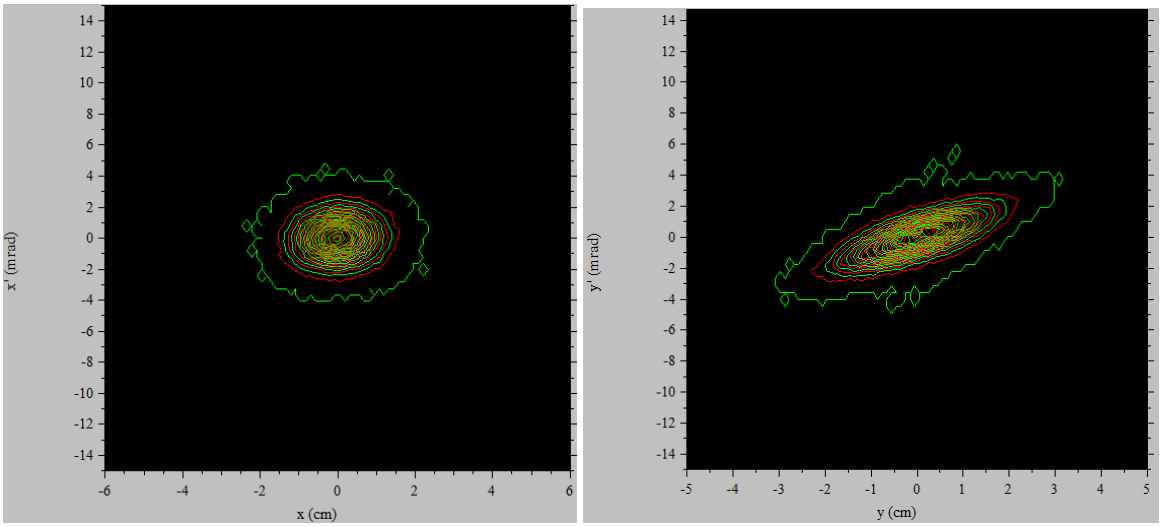

Figure 21: Horizontal (right) and vertical (left) phase ellipses for a S3 central field of 1.4 kG.

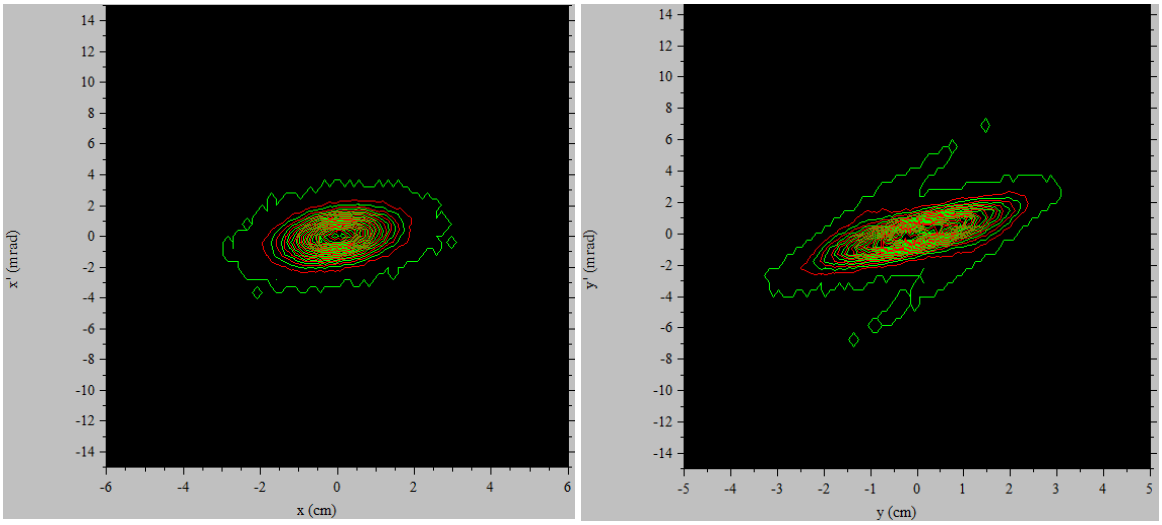

Figure 22: Horizontal (right) and vertical (left) phase ellipses for a S3 central field of 1.5 kG.

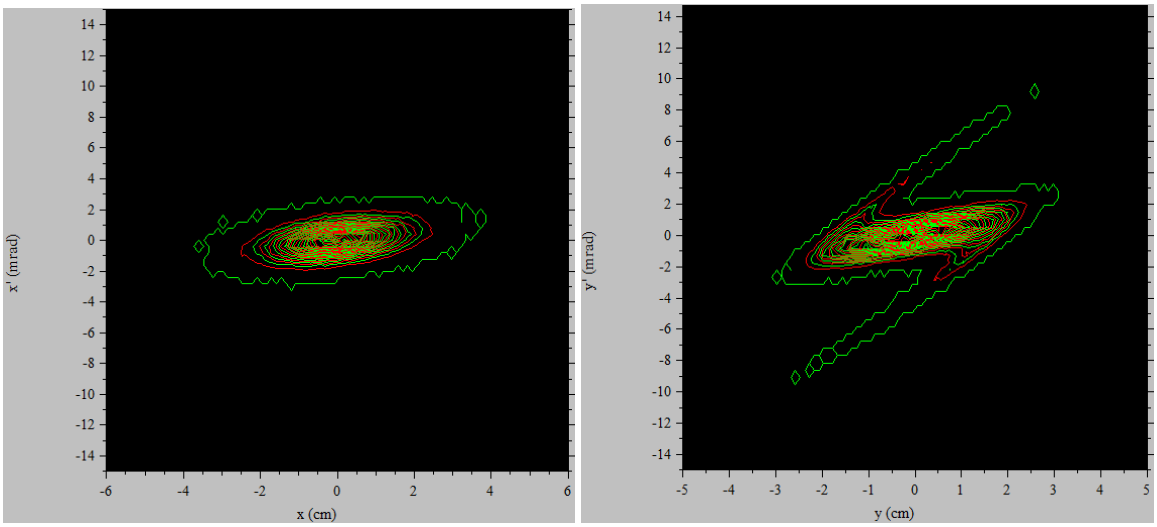

Figure 23: Horizontal (right) and vertical (left) phase ellipses for a S3 central field of 1.6 kG.

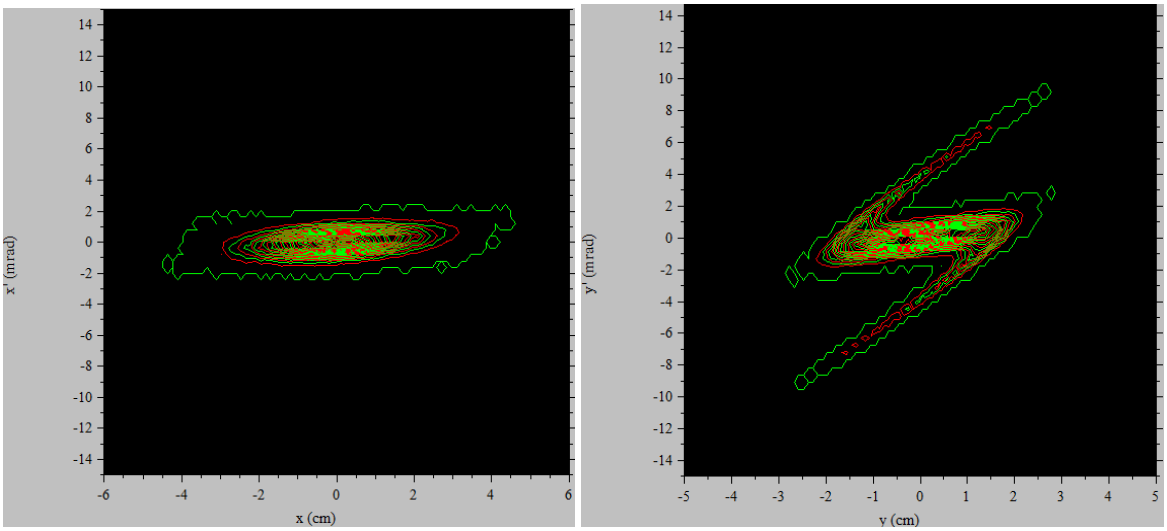

Figure 24: Horizontal (right) and vertical (left) phase ellipses for a S3 central field of 1.7 kG.

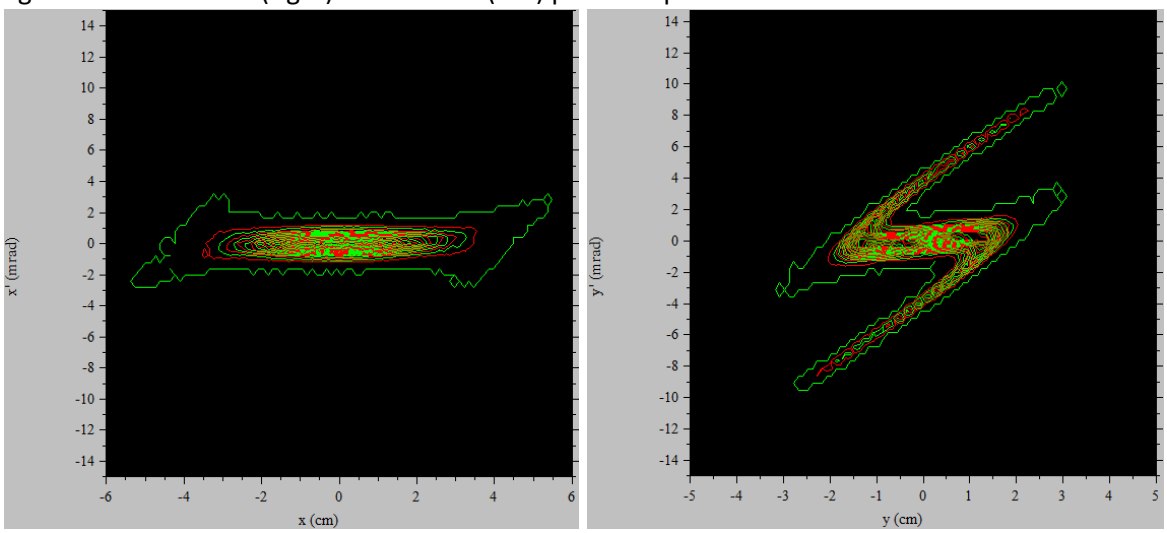

Figure 25: Horizontal (right) and vertical (left) phase ellipses for a S3 central field of 1.8 kG.

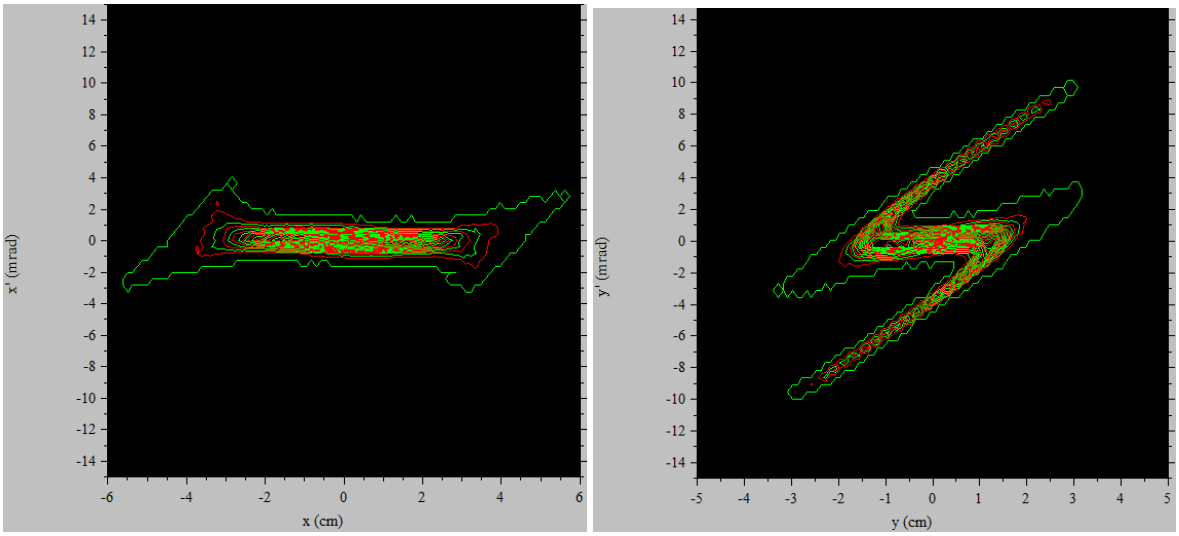

Figure 26: Horizontal (right) and vertical (left) phase ellipses for a S3 central field of 1.9 kG.

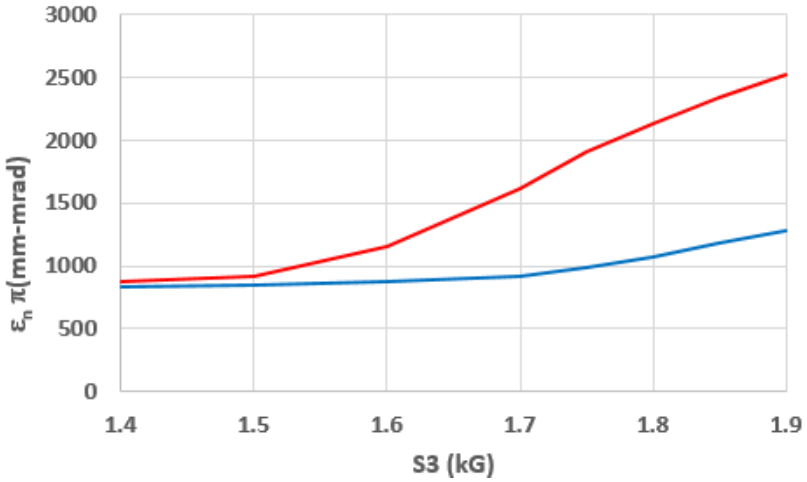

Figure 27: Predicted normalized emittance at Station C as a function of S3 peak field. The blue and red curves are the emittance in the horizontal and vertical planes respectively.

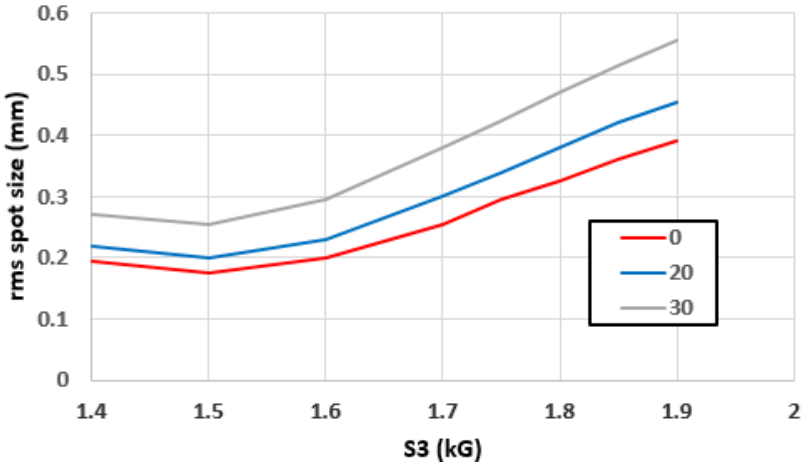

Figure 28: RMS spot size on target for different S4 magnet settings in amperes as a function of the S3 field

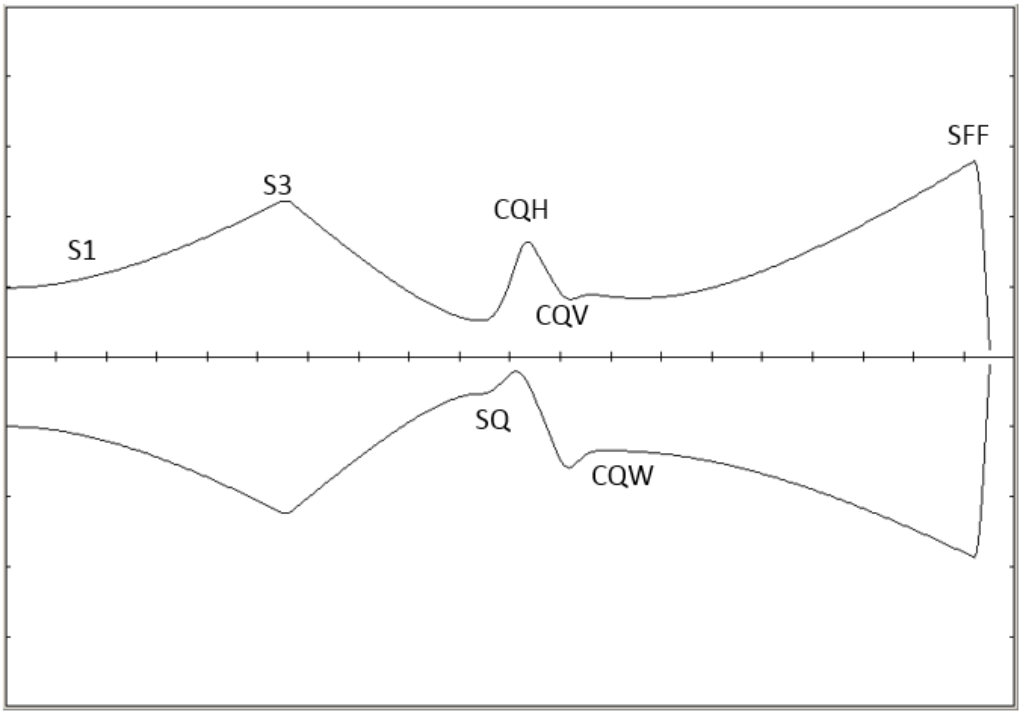

Conclusions

A major source of emittance growth in the DARHT-II accelerator has been identified. The need to expand the beam for 4-pulse radiography in order to suppress ions and rf from the septum dump exposes the beam to significant nonlinear fields in the Collins quadrupoles. The measured beam profiles at station C are shown to be the result of the nonlinear fields in the Collin quadrupoles. The duodecapole filed is the most dominant multipole. The increases in the emittance and the spot size on target due to these aberrations are substantial.

REFERENCES

[1] PSI Graphic Transport Framework by U. Rohrer based on a CERN-SLAC-FERMILAB version by K.L. Brown et al., K.L Brown, D.C. Carey, Ch. Iselin, and F. Rothacker, "TRANSPORT A Computer Program for Designing Charged Particle Beam Transport Systems," SLAC-91 (1973 Rev.), NAL-91, and CERN 80-4.

[2] PSI Graphic Turtle Framework by U. Rohrer based on a CERN-SLAC-FERMILAB version by K.L. Brown et al., TURTLE

[3] M. Schulze, LA-CP-16-20309, "A Study of the Contribution of Kicker Pulse Non-Uniformity to the Spot Size at the X-ray Converter Target".

[4] M. Schulze et al, "Ion Production and RF Generation in the DARHT-II Beam Dump", LA-UR-13-23509, 2013 IEEE Pulsed Power & Plasma Science Conference.

[5] D. Barlow, "tests and Measurements of the Collins Quads for DARHT", LANSCE-ABS:06-004 (TN), 9-January-2006.

[6] POISSON, K. Halbach, "A Program for Inversion of System Analysis and Its Application to the Design of Magnets," Lawrence Livermore National Laboratory report UCRL-17436 (1967); CONF-670705-14.